CrossMark

ORIGINAL PAPER

Azolla pinnata: An Efficient Low Cost Material for Removal of Methyl Violet 2B by Using Adsorption Method

Muhammad Raziq Rahimi Kooh[1] · Linda B. L. Lim[1] · Muhammad Khairud Dahri[1] ·
Lee Hoon Lim[1] · J. M. R. Sarath Bandara[1]

Abstract *Azolla pinnata* (*AP*), a floating aquatic macrophyte, was studied as a potential adsorbent for the removal of methyl violet (MV) in a batch adsorption system. Surface characterisation, effects of particle size, adsorbent dosage, pH, ionic strength and pre-treatments of adsorbent were carried out. The study of the effects of pH and ionic strength suggested that electronic interaction and hydrophobic–hydrophobic interaction might be the major forces of dye interaction. Pseudo 2nd order kinetic model best-fitted the kinetic data indicating that the adsorption process may be controlled by chemical process. The Weber–Morris and Boyd models were used for describing the diffusion mechanism which showed that intraparticle diffusion was not the rate limiting step, and film diffusion or in combination of other mechanisms might be in control. Isotherm modelling showed that the Langmuir model best-fitted the experimental data with q_m of 194.2 mg g^{-1} at 25 °C and 323.4 mg g^{-1} at 65 °C. Thermodynamic studies showed that the adsorption process is endothermic, spontaneous and with significant change to the internal structure of adsorbent. The estimated activation energy by Arrhenius equation is 54.8 kJ mol^{-1}, which indicates that the adsorption process may be controlled by chemical process. Adsorbent regenerated using NaOH displayed retention of high adsorption capability almost similar to fresh adsorbent even after five consecutive cycles. Ability to regenerate coupled with good adsorption capability suggests that *AP* has great potential to be utilised as a low-cost adsorbent for the removal of MV in real life application.

Keywords *Azolla pinnata* · Low cost adsorbent · Methyl violet 2B · Adsorption · Kinetic studies · Regeneration

Disclaimer This study investigate the potential of the freshwater aquatic fern *Azolla pinnata* in the removal of the methyl violet 2B. However *Azolla pinnata* is an invasive species and may be illegal to possess in certain countries. To use *Azolla pinnata* for whatsoever purposes required proper planning and approval with relevant authorities or organizations therefore the authors will not be held accountable for any liabilities incurred from whatsoever usage derived from this work.

✉ Muhammad Raziq Rahimi Kooh
chernyuan@hotmail.com

Linda B. L. Lim
linda.lim@ubd.edu.bn

Muhammad Khairud Dahri
kiddri86@hotmail.com

Lee Hoon Lim
leehoon.lim@ubd.edu.bn

J. M. R. Sarath Bandara
bandara.sarath@gmail.com

[1] Faculty of Science, Universiti Brunei Darussalam, Jalan Tungku Link, Pengkalan Gadong, Bandar Seri Begawan 1410, Brunei

Introduction

Synthetic dyes are extensively used in the current era, but they are considered as one of the pollutants that raises concerns due to its impact on the environment as well as its toxic effect on living things. Due to their xenobiotic nature and stability, synthetic dyes are recalcitrant to biodegradation, and are highly visible even in low level contamination. The water bodies, where dyes are discharged, exhibit low biological oxygen demand (BOD) and high chemical oxygen demand (COD) [1]. Furthermore, the dyes can interfere with aquatic ecosystem as they can hinder photosynthetic activity and upset the biological processes [2].

Decolourisation techniques such as the uses of oxidising or reducing agents, biological methods (live plant, fungi or

microorganism such as bacteria), electrochemical degradation, ion-exchange, irradiation, precipitation, reverse osmosis and adsorption methods were conventional methods of wastewater treatment. The advantages and disadvantages of these methods are widely discussed in the literatures [3–5].

Adsorption method is one of the preferred ways of wastewater treatment due to its simplicity in design and usually does not produce harmful side-products [6]. Another attractive feature of this treatment is that the materials used are often abundant in nature such as *Causarina equisetifolia* needle [7], peat [8], and agricultural residues e.g. rice husk [9], peanut hulls [10], sugarcane bagasse [11, 12], tarap fruit peel [13] and walnut shell [14], and this resulted in lower cost of treatment. The adsorbent can also be physically modified by heat treatment and autoclaved [15], or chemically modified via various methods, such as immobilisation with sodium alginate [16], mineral acid treatment with hydrochloric acid [11, 12] or sulphuric acid [15], and treatment with chelating agents e.g. polyethyleneimine [12, 17], to increase the dye adsorption capacity.

Methyl violet 2B (MV) is a popular purple colour dye used in textile industry, paper printing, and it is also an active ingredient in Gram's biological stain for bacteria classification [18]. However, MV is known to cause severe irritation to skin, eye, respiratory tract and gastrointestinal tract.

The primary aim of this study is to investigate the potential usage of water fern, *Azolla pinnata* (AP), as an adsorbent for the removal of MV dye. The AP is an invasive freshwater aquatic fern that contains nitrogen-fixing cyanbacteria, *Anabaena azollae,* as its symbiont which leads to rapid colonisation of water bodies. Uncontrolled proliferation of AP leads to the formation of dense mat of aquatic fern and the greening of the water (caused by algal bloom of free-living *Anabaena azollae*) which reduce light penetration into the water. These effects can reduce photosynthetic activity of the submerged aquatic plants and rapid depletion of dissolved oxygen concentration in the water [19]. This can potentially cause harm to the aquatic life. In view of the proliferous growth of AP in association with *Anabaena azollae* in tropical water bodies with least of attention and input, the main objective of this study was to evaluate the ability of AP as a substrate for remediation of MV in water bodies.

Materials and Methods

Chemicals and Reagents

Biological stain grade methyl violet 2B dye (MV) ($C_{24}H_{28}N_3Cl$; M_r 393.95 g mol^{-1}), with purity of 80 % dye content was purchased from Sigma Aldrich Corporation. pH of solution was adjusted using NaOH and HNO$_3$ which were

purchased from Fluka. Spectroscopy grade KBr was used for FTIR analysis and was dried in oven at 110 °C before use. Chemical reagents used for pre-treatment of adsorbent include oxalic acid (99 % purity, Harris Reagent), 85 % phosphoric acid (ACS grade for analysis, Merck) and citric acid (99 % purity, BDH). All chemical were used without further purification.

Adsorbent and Stock Preparation

Azolla pinnata (AP) was obtained from the Agriculture Department, Ministry of Industrial and Primary Resource, Brunei Darussalam. The AP was grown under natural light in plastic containers using water from freshwater fishpond. Multiple harvesting of the AP were carried out over a period of three months and the AP was washed several times with distilled water followed by oven-dried at 75 °C until a constant weight was obtained. Dried samples were ground to fine powder using mortar and pestle and sieved to obtain various particle sizes (>850 μm, 355–850 and <355 μm) and were stored in a desiccator. MV stock solution of 1000 mg L^{-1} was prepared by dissolving the required amount of MV solid in distilled water. The stock solution was then used to prepare solution of various concentrations. All experiments were carried out in duplicates.

Instrumentation

The absorbance of dye solution was measured at optimum wavelength, λ_{max}, of 584 nm using a single beam UV–vis spectrophotometer (Jenway 6320D spectrophotometer). The elemental CHNS composition of AP was determined using a Thermo Scientific Flash 2000 Organic Elemental Analyzer CHNS/O. Fourier Transform Infrared (FTIR) spectrophotometer (Shimadzu Model IRPrestige-21) was used to characterise the functional groups present in the untreated AP and MV-treated AP. X-ray fluorescene (XRF) spectrophotometer (PANalytical Axios^{max}) was used to determine the percentage of elements present in the AP and MV-treated AP. Prior to scanning electron microscope (SEM) imaging, the surface coating of the samples were carried out using an SPI-Module 1143 Sputtering Coater, at plasma current 15 mA for 120 s. SEM images of untreated AP and MV-treated AP were obtained using JEOL JSM-5800LV (Japan), under high vacuum mode and accelerating voltage of 15 kV. Stuart orbital shaker was used for agitation of the solution. Thermo Scientific Orion 2 Star pH Benchtop was used to measure the pH.

Point of Zero Charge

The pH$_{pzc}$ of the adsorbent was determined by the salt addition method using 0.1 M KNO$_3$ solutions [20]. The

initial pH (2.5–10.0) of 20 mL KNO_3 was adjusted using 0.1 M HNO_3 and NaOH, and the pH was measured. 0.04 g adsorbent was added and agitated for 24 h and the final pH was measured. The pH_{pzc} was obtained by plotting the change in pH (final pH—initial pH) versus initial pH.

Batch Experiment Procedures

Batch experiments were carried out by mixing 0.04 g of adsorbent with 20.0 mL of known concentration of MV in a 150 mL Erlenmeyer flask. The mixtures were agitated using orbital shaker at 250 rpm at room temperature. Parameters such as particle size (sieve sizes: >850, 355–850 and <355 μm), adsorbent dosage (0.01–0.10 g), contact time (5–240 min), initial concentration (20–1000 mg L^{-1}), pH (3.0–8.0), temperature (ambient, 35, 45, 55, 65 °C), and ionic strength were investigated. The mixture was filtered and the filtrates were analysed using an UV–vis spectrophotometer. The experiments were carried out under agitation time of 120 min unless otherwise stated.

The amount of MV adsorbed per gram of AP, q_e (mg g^{-1}), was calculated by the following equation:

$$q_e = \frac{(C_i - C_e)V}{m} \tag{1}$$

where C_i is the initial dye concentration (mg L^{-1}), C_e is the equilibrium dye concentration (mg L^{-1}), V is the volume of MV solution used (L) and m is the mass of AP used (g). The percentage removal of the dye represent by:

$$\text{Percentage removal} = \frac{(C_i - C_e) \times 100\,\%}{C_i} \tag{2}$$

The adsorption process was described using the Langmuir, Freundlich and Dubinin-Radushkevich isotherm models.

Error Analysis

The kinetic and isotherm models that best fit the equilibrium data were determined by the values of the coefficient of determination (R^2). In addition, the predicted q_e ($q_{e,cal}$) were calculated from either the kinetic or isotherm models and error analyses were applied. Best fit of experimental data ($q_{e,exp}$) was determined by the smallest values of these error analyses functions which indicates the least error [21].

The equations of the four types of error analysis are as follows:

$$\text{Sum of absolute error (EABS)}: \sum_{i=1}^{n} |q_{e,exp} - q_{e,cal}| \tag{3}$$

$$\text{Chi-square test}\,(\chi^2): \sum_{i=1}^{n} \frac{(q_{e,exp} - q_{e,cal})^2}{q_{e,exp}} \tag{4}$$

$$\text{Average relative error (ARE)}: \frac{100}{n} \sum_{i=1}^{n} \left| \frac{q_{e,exp} - q_{e,cal}}{q_{e,exp}} \right|_i \tag{5}$$

Marquardt's percent standard deviation (MPSD):

$$100 \sqrt{\frac{1}{n-p} \sum_{i}^{n} \left(\frac{q_{e,exp} - q_{e,cal}}{q_{e,exp}} \right)^2} \tag{6}$$

where $q_{e,exp}$ is the experimental value while $q_{e,cal}$ is the calculated value, n is the number of data points in the experiment and p is the number of parameters of the isotherm model.

Regeneration Experiment

The regeneration experiments were examined for three different types of solvents: distilled water, 0.1 M HNO_3 and 0.1 M NaOH. Three sets of adsorbent were treated with 100 mg L^{-1} MV to obtained MV-treated AP at the dosage of 0.04 g/20 mL dye. The MV-treated AP was washed with distilled water and shaken in an orbital shaker for 30 min. The washed solution was discarded and the same procedure was repeated until little desorption of dye from the adsorbent into the distilled water. The solid was subsequently dried in oven at 70 °C. Similar procedure was applied to the acid and basic wash, where 20 mL of 0.1 M acid or base added, shaken for 30 min and followed by multiple distilled water washing until pH of the washed solution became near neutral.

Pre-treatment of Adsorbent

AP was subjected to various treatments to assess its adsorption ability and to investigate if such treatment could enhance its adsorption capacity when compared to the untreated adsorbent. The treatment of adsorbent was based on literatures, with some alterations of the procedure.

Briefly, adsorbent was treated with 1.0 M oxalic acid [22] and 0.06 M citric acid [23] at dosage of 10 mL chemical reagent per gram adsorbent and agitated in an orbital shaker for 2 h. Chemical-treated adsorbent was filtered with a Whatman No. 41 filter paper and dried at 60 °C for 24 h. It was heated at 120 °C in an oven for 2 h, followed by 0.05 M $NaHCO_3$ washing, and then repeatedly with distilled water until the pH of effluent was near neutral, and dried at 60 °C.

The chemical treatment with phosphoric acid was carried out at dosage of 10 mL 85 % H_3PO_4 per gram adsorbent, and was agitated for 2 h and left to stand for 24 h at room temperature [24]. The washing procedure is similar

to the oxalic acid and citric acid method as mentioned earlier.

NaOH-treated adsorbent was prepared at the dosage of 10 mL 1 M NaOH per gram adsorbent, agitated for 2 h, washing with distilled water washing until the effluent is near neutral, and dried in an oven at 60 °C [25].

Adsorption capacity of modified adsorbents was investigated at dosage of 0.02 g/20 mL dye at ambient pH.

Results and Discussion

Characterisation of Absorbent

The C, H, N, S compositions of AP on dry weight were 44.18, 6.27, 4.01 and 0.20 % respectively. The XRF elemental analyses of AP before and after dye treatment are as shown in Table 1. After dye treatment, the K and Na contents showed reduction from 14.39 and 4.38 % to 0.19 and 0.14 %, respectively. Such observation could be attributed to the K^+ and Na^+ ions being displaced by MV, which is a cationic dye. Similar findings were reported for the adsorption of basic dyes using tarap peel and peat soil [13, 26].

The FTIR spectra of untreated AP and MV-treated AP are shown in Fig. 1. The FTIR spectrum of the untreated AP indicates the presence of various functional groups at wavelengths 3279 cm^{-1} (O–H stretch), 2918 cm^{-1} and 2849 cm^{-1} (C–H stretch), 1651 cm^{-1} (C=O bending) and 1033 cm^{-1} (out-of-plane bending of carbonate). FTIR spectrum of MV-treated AP displayed bands at 3319 cm^{-1} (O–H stretch), 2918 cm^{-1} and 2849 cm^{-1} (C–H stretch), 1658 cm^{-1} (C=O bending) and 1026 cm^{-1} (out-of-plane bending of carbonate), where the shift of the bands may indicate that these functional groups interact with the MV molecules [9, 27]. The three bands that are present only on MV-treated AP are 1587 cm^{-1} (–COO$^-$ anti-symmetric stretching), 1365 cm^{-1} (–COO$^-$ symmetric stretching) and

1173 cm^{-1} (C–N stretching of MV) confirmed the loading of MV dye into the adsorbent [9]. This data also suggested that functional groups of –COO$^-$ may be responsible for the interaction between the adsorbent and the dye molecules [9].

The SEM images of untreated and MV-treated AP are as shown in (A) and (B) of Fig. 2, respectively. These images showed that the adsorbent particle surface is rough in nature and no obvious distinction can be found between the adsorbent particles of untreated and MV-treated AP.

Effect of Particle Size and Adsorbent Dosage

The three particles sizes, >850 μm, 355–850 and <355 μm, resulted in dye removal of 60.8, 87.2 and 92.4 % respectively. The smaller the particle size, the higher the surface area and hence more functional groups are exposed for the interaction with dye molecules. As particle size of <355 μm gave the highest percentage removal, thus particle of this size was used for the rest of the experiment.

The effect of adsorbent dosage on removal of MV is shown in Fig. 3. The removal of MV increases when the dosage was increased from 0.01 to 0.04 g and no further increase beyond 0.04 g was observed. Therefore, 0.04 g is taken as the optimum dosage and subsequently used for the rest of the experiment.

Effect of Contact Time and Concentration

Determination of the contact time between AP and the MV is essential in adsorption experiment as it ensures that the dye uptake by the AP reaches a saturation point where there will be no significant net transfer of dye between the AP and the solution beyond that point. The effect of contact time on the adsorption of MV by AP at different initial dye concentrations (C_i = 100, 200, 300, 400 mg L^{-1}) is shown in Fig. 4a.

Rapid dye uptake occurred within the first 30 min of contact time and the uptake gradually slowed down until it became constant. The rapid initial MV uptake is due to the availability of large amount of vacant sites at the beginning of the adsorption process, which gradually become less available and more difficult over time due to the build-up of the repulsion forces between the dye molecules in the solid and bulk phases [28]. As seen in Fig. 4a and 4c, higher C_i resulted in higher dye uptake because high C_i provides the driving force that overcome the resistances and transfer the dye molecules deeper into the micropores of the adsorbent [28].

The time taken to reach equilibrium for C_i at 100, 200, 300 and 400 mg L^{-1} were 60, 60, 90 and 120 min, respectively.

Table 1 XRF data of AP before and after treatment of MV

Elements	Normalised percentage (%)	
	Before	After
Al	0.45	0.39
Mn	0.49	0.35
P	2.48	1.02
Mg	3.66	2.64
Na	4.38	0.14
Cl	8.65	1.03
Ca	12.31	10.71
K	14.39	0.19
O	28.47	29.62

Fig. 1 FTIR spectra of A untreated AP and B MV-treated AP
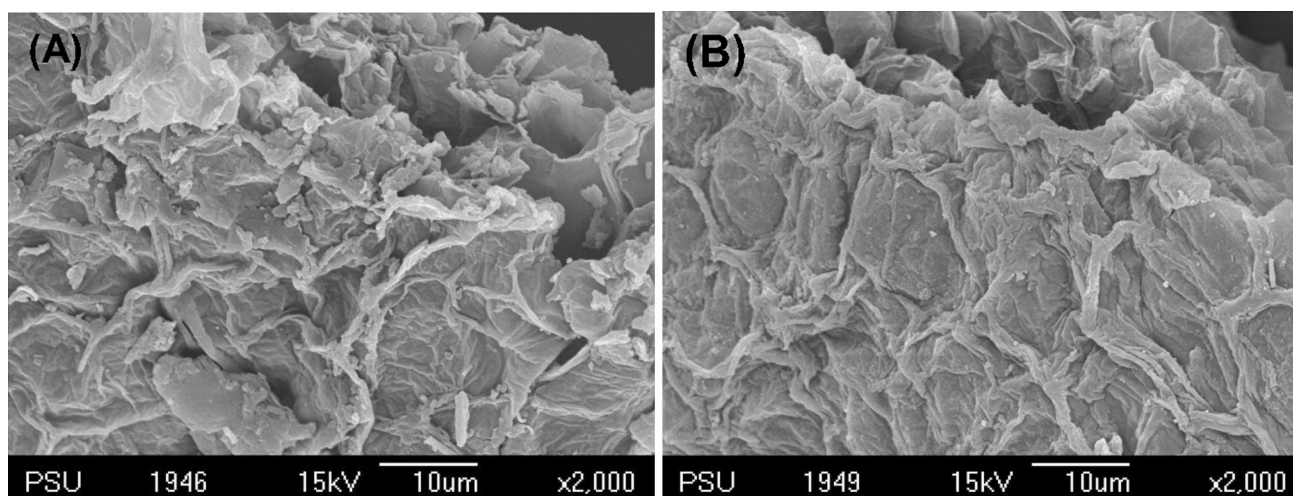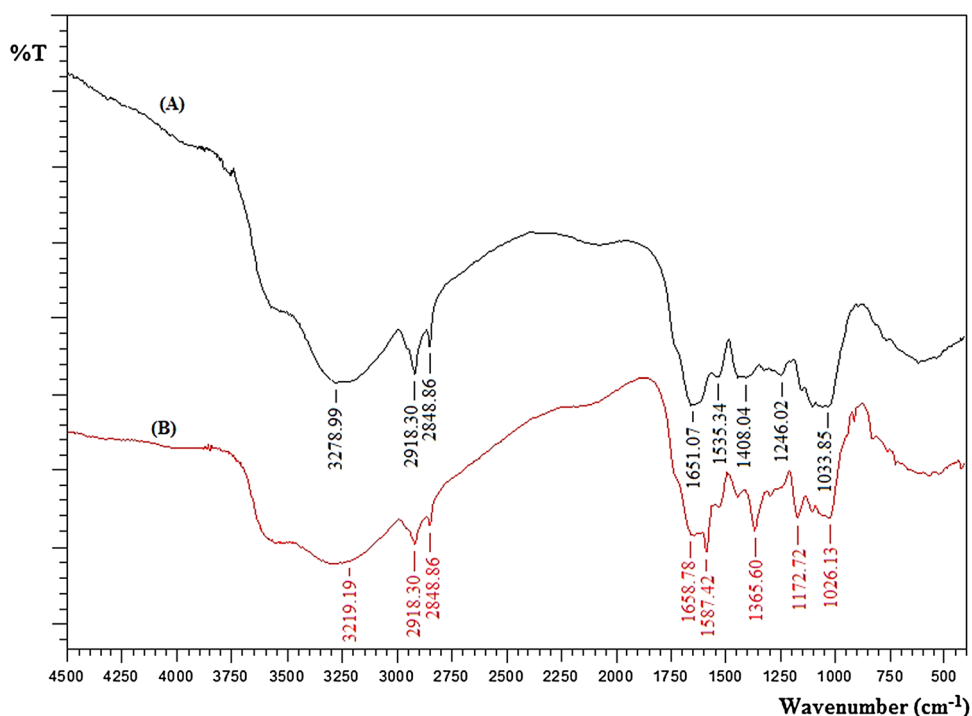

Fig. 2 SEM images of **a** untreated AP, and **b** MV-treated AP treated, at ×2000 magnification

Thus, agitation time of 120 min was chosen for all the experiments, to ensure complete equilibrium was attained.

The effect of temperature on dye uptake on 100 mg L^{-1} MV is shown in Fig. 4b. It can be observed that the dye uptake was more rapid at higher temperature and the equilibrium was attained within the first 30 min. Higher temperature (35–55 °C) also resulted in higher q_e at equilibrium point, while adsorption beyond 55 °C did not result in any increase of q_e. Further analysis of thermodynamic data using the Arrhenius equation was discussed under the "Thermodynamic Studies" section.

Kinetic Studies

In this study, four widely used kinetics models, namely the Lagergren 1st order [29], pseudo 2nd order [30], Weber-Morris intraparticle diffusion [31] and Boyd [32] models were used in characterising the adsorption mechanism between the dye and the adsorbent.

The Lagergren 1st order is expressed as:

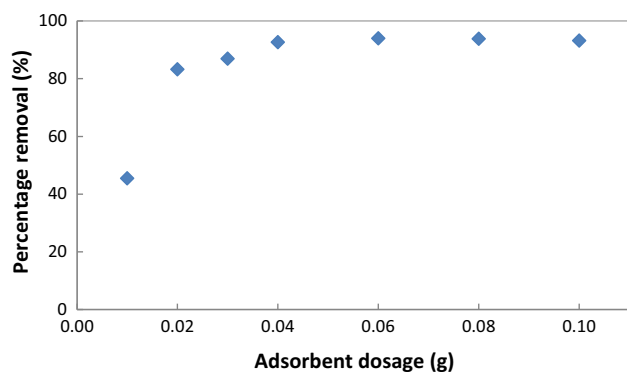$$\log(q_e - q_t) = \log q_e - \frac{t}{2.303}K_1 \qquad (7)$$

Fig. 3 Effect of adsorbent dosage on the removal of 100 mg L^{-1} MV, with total volume of mixture at 20 mL
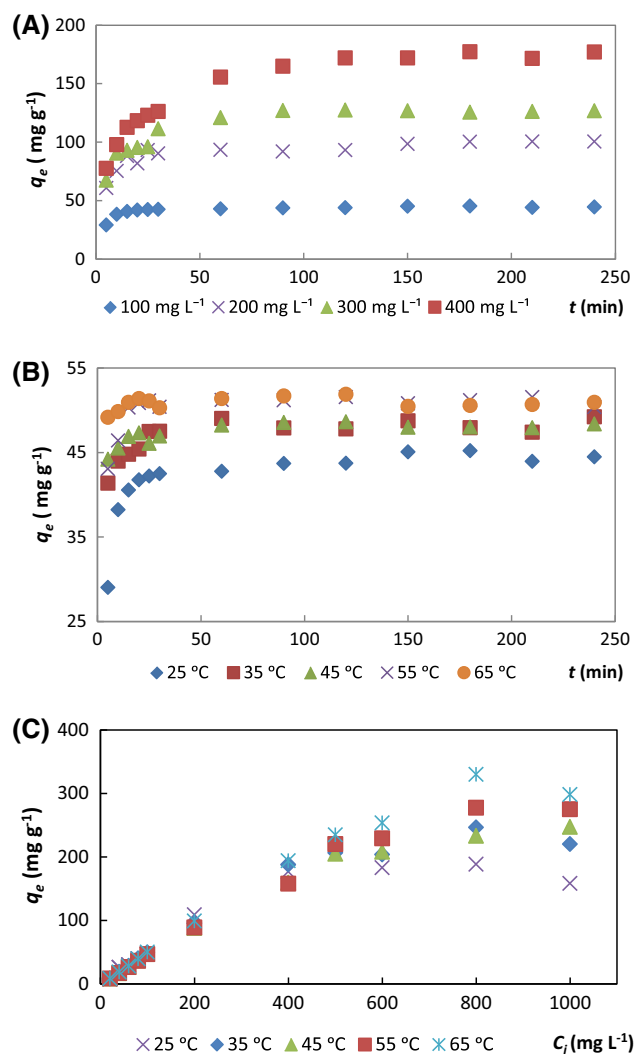

Fig. 4 Effect of contact time at **a** different initial dye concentrations (100, 200, 300, 400 mg L^{-1}) at ambient temperature of 25 °C, **b** different temperature (25, 35, 45, 55, 65 °C) at C_i 100 mg L^{-1} MV, and **c** effect of concentration of MV adsorption at different temperature

where q_t is the amount of MV adsorbed per gram of *AP* (mg g^{-1}) at time t, K_1 is the Lagergren 1st order rate constant (min^{-1}) and t is the time shaken (min).

The pseudo 2nd order is expressed as:

$$\frac{t}{q_t} = \frac{1}{q_e^2 K_2} + \frac{t}{q_e} \tag{8}$$

where K_2 is pseudo second order rate constant (g mg^{-1} min^{-1}).

The rate constant K_1, K_2 and the $q_{e,\text{cal}}$ (predicted adsorbate concentration at equilibrium) were obtained from the linear plot of $ln(q_e - q_t) vst$ and $\frac{t}{q_t} vst$, respectively.

The parameters of Lagergren 1st order and pseudo 2nd order are summarised in Table 2. The values of R^2 of the kinetic models are higher for pseudo 2nd order ($R^2 \geq 0.999$) (Fig. 5a) as compared to the Lagergren 1st order for C_i of 100, 200, 300 and 400 mg L^{-1}. The calculated adsorption capacity ($q_{e,\text{cal}}$) of the pseudo 2nd order is closer to the experimental adsorption capacity ($q_{e,\text{exp}}$) than that of Lagergren 1st order. For example, using 100 mg L^{-1} the $q_{e,\text{cal}}$ for pseudo 1st and 2nd order are 23.7 and 48.9 mg g^{-1}, respectively, while the $q_{e,\text{exp}}$ is 47.2 mg g^{-1}, clearly indicating that the adsorption follows the pseudo 2nd order. This is further supported by the error analyses functions (χ^2, ARE, EABS and MSDP) where the pseudo 2nd order showed the lowest values which indicates the least error. Therefore with consideration of the R^2, $q_{e,\text{cal}}$ and the values of error analyses function, it is concluded that the pseudo 2nd order best fit the data, and the adsorption process may be governed by chemical process.

Weber-Morris intraparticle diffusion model was used for describing the diffusion mechanism, as this mechanism is not applicable to Lagergren 1st order and pseudo 2nd order models. Typically, the diffusion process of the adsorbate can be classified into three phases. The first phase is a fast external diffusion or the boundary layer diffusion, followed by the gradual surface adsorption owning to the intraparticle diffusion, and lastly, the slow equilibrium phase [33, 34].

The equation of the Weber-Morris intraparticle diffusion model is expressed as:

$$q_t = K_3 t^{1/2} + C \tag{9}$$

where K_3 is the intraparticle diffusion rate constant (mg g^{-1} min$^{-1/2}$) and C is the intercept.

The parameters K_3 and C were determined from the linear plot of q_t versus $t^{1/2}$.

The Weber-Morris plot is as shown in Fig. 5b, where multi-linearity is observed, and the parameters are summarised in Table 2. The fast external diffusion was completed very rapidly within 5 min and thus it is not observed in the Weber-Morris plot. Similar behaviour was observed by

Table 2 Parameters of the kinetic models of various concentrations at ambient temperature

Lagergren 1st order model				
C_i (mg L^{-1})	100	200	300	400
$q_{e,cal}$ (mg g^{-1})	23.7	34.7	33.9	76.1
$q_{e,exp}$ (mg g^{-1})	47.2	100.3	127.3	177.2
K_1	0.032	0.027	0.021	0.016
R^2	0.972	0.814	0.714	0.881
χ^2	135.4	646.5	864.6	907.8
EABS	209.2	860.7	1060.4	1276.7
ARE	45.1	74.9	75.8	72.0
MSDP	74.9	82.1	90.4	79.4
Pseudo 2nd order model				
$q_{e,cal}$ (mg g^{-1})	48.9	101.5	130.1	183.6
$q_{e,exp}$ (mg g^{-1})	47.2	100.3	127.3	177.2
K_2	0.003	0.002	0.001	0.001
R^2	0.999	0.999	0.999	0.999
χ^2	1.3	3.4	2.9	5.9
EABS	13.6	45.8	42.6	61.1
ARE	3.5	4.3	3.4	4.3
MSDP	8.3	6.2	5.6	7.8
Weber-Morris Intraparticle diffusion model				
Region A				
K_{3a} (mg g^{-1} min$^{1/2}$)	6.585	10.689	10.918	14.977
C_a	7.6	39.7	48.1	48.7
R^2	0.889	0.901	0.846	0.948
Region B				
K_{3b} (mg g^{-1} min$^{1/2}$)	0.999	0.944	1.238	4.354
C_b	33.9	85.7	110.1	115.9
R^2	0.841	0.779	0.605	0.774
Boyd Model[a]				
Slope	0.032	0.032	0.045	0.024
Intercept	0.191	0.701	0.108	0.064
R^2	0.972	0.975	0.965	0.995

[a] Parameters calculated from the initial linear region of the plot only

Özacar and Şengil in the adsorption of disperse dye onto alunite [34] and the adsorption of phosphate into red mud [33]. The initial region in Fig. 5b represented the gradual surface adsorption owning to intraparticle diffusion phase, while the plateau region represented the slow equilibrium phase. According to the Weber-Morris model, if the linear plot passes through the origin, then the intraparticle diffusion is the rate-limiting step. As shown in Table 2, the values of C (intercept) were non-zero, which indicate that intraparticle diffusion was not the rate-limiting step and other mechanisms may be involved. The C value is associated with the thickness of the boundary layer, and the larger C value may represent thicker boundary layer.

The kinetic data was analysed with the Boyd model to further determine the diffusion mechanism of the adsorption
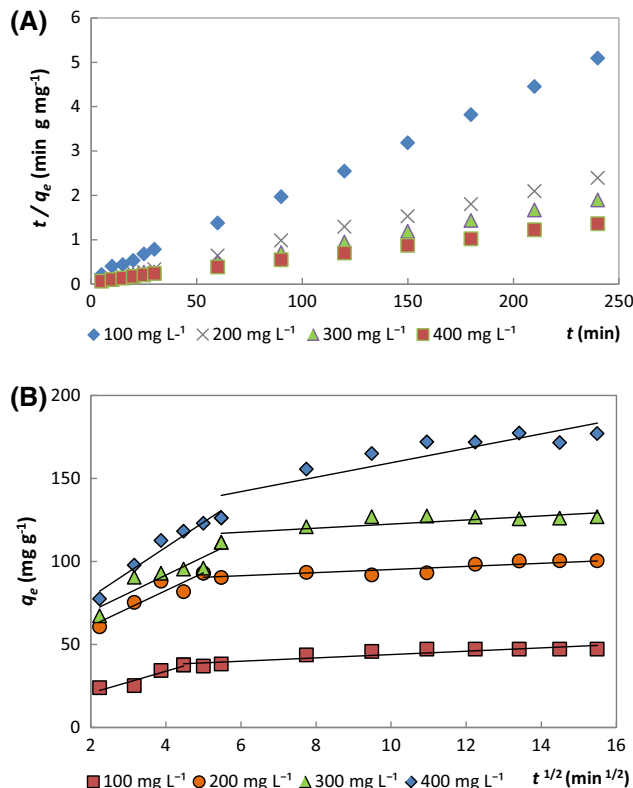
(A)

(B)

Fig. 5 Plot of **a** pseudo 2nd order kinetic model, and **b** Weber-Morris model displayed multi-linearity behavior, for C_i of 100, 200, 300 and 400 mg L^{-1} MV adsorption by *AP* at dosage of 0.04 g/20 mL dye, at room temperature and ambient pH

process. The Boyd model can be used to identify whether the adsorption process is governed by film diffusion or particle diffusion. Film diffusion is the transport of adsorbates to the external surface of adsorbent, while particle diffusion is the transport of adsorbates within the pores of the adsorbent [35].

The Boyd model is expressed as:

$$B_t = -0.4977 - \ln(1 - F) \tag{10}$$

where F is equivalent to q_t/q_e, and B_t is mathematical function of F.

The slopes and intercepts of the linear plot of B_t versus t was summarised in Table 2. In our study, multilinearity was also observed for the Boyd plot (plot not shown), only the first linear region (q_t 5–30 min) was used for the calculation of the parameters (slope and intercept) [36]. According to the Boyd model, if the linear plot passes through the origin, then the diffusion is controlled by particle diffusion, otherwise it is controlled by film diffusion [35]. As all the values of the Boyd plot intercept are non-zero, this indicates that the diffusion may be controlled by film diffusion or in combination with other mechanisms.

Effects of pH and Ionic Strength

It is well established that adsorption of the dye molecules by adsorbent is mainly by electrostatic interaction, hydrophobic–hydrophobic interaction and hydrogen bonding, and pH affect mainly the electrostatic interaction [37, 38].

Prior to the investigation of the effect of pH on adsorption activity of *AP*, it is essential to determine the range of pH where the colour intensity of the dye MV will not be affected. As MV is used as pH indicator for low acidic region, the pH region where the colour of MV changes from purple to green and yellow needs to be avoided. The pH range from 2.0 to 12.0 was investigated. The decrease of colour intensity was observed at extreme pH from 11.0 to 12.0, which may be due to alkaline fading [39]. Reduction of colour intensity was also observed at pH <3.0 which may be due to formation of MV-H^{2+} species, which was observed for another basic dye (malachite green) of same triarylmethane dye category as MV [39]. Therefore the study of the adsorption of MV by *AP* was limited to range of pH 3.0–10.0.

The effect of pH on dye adsorption by *AP* is summarised in Fig. 6a. The optimum pH of MV adsorption by the *AP* is pH 4.0 at 54.1 mg g^{-1} (94.0 % removal), while ambient pH of 5.4 resulted in q_e of 51.5 mg g^{-1} (93.5 % removal). The differences of dye adsorption between the optimum pH and the ambient pH are insignificant thus all the adsorption experiments were carried out at the ambient pH of 5.4.

The point of zero charge (pH_{pzc}) of *AP* was found to be at pH 6.6. Using the concept of pH_{pzc}, the surface of *AP* will be predominant negatively charged when solution pH > 6.6, while predominant positively charged when pH < 6.6. As MV is a cationic dye, the predominant positively charged surface of *AP* at pH < 6.6 should be unfavourable for adsorption of MV due to electronic repulsion. However, as observed in Fig. 6a, that pH 3.0–6.0 showed high removal which is not significantly different from adsorption at pH 8.0 and 10.0. This indicates that the adsorption system of *AP* and MV is not limited to only the electronic interaction. This is further verified by the study on the effect of ionic strength on the adsorption of MV by *AP*.

Solutions of KNO$_3$, NaCl and MgSO$_4$ were used to study the effect of salt content (concentration 0.01–0.90 M) on the adsorption process of MV by *AP*. Salt concentration is directly proportionally to the ionic strength and thus a higher salt concentration will result in a higher ionic strength. As seen in Fig. 6b, all the three salts (KNO$_3$, NaCl and MgSO$_4$) resulted in the decrease of MV adsorption as the ionic strength increase. This behaviour is usually observed for adsorption of basic dye in high ionic strength condition [14, 37]. At 0.9 M of KNO$_3$, NaCl and MgSO$_4$, the q_e was reduced from approximately 47.0 mg g^{-1}, to 27.0, 39.2 and 36.7 mg g^{-1}, respectively.
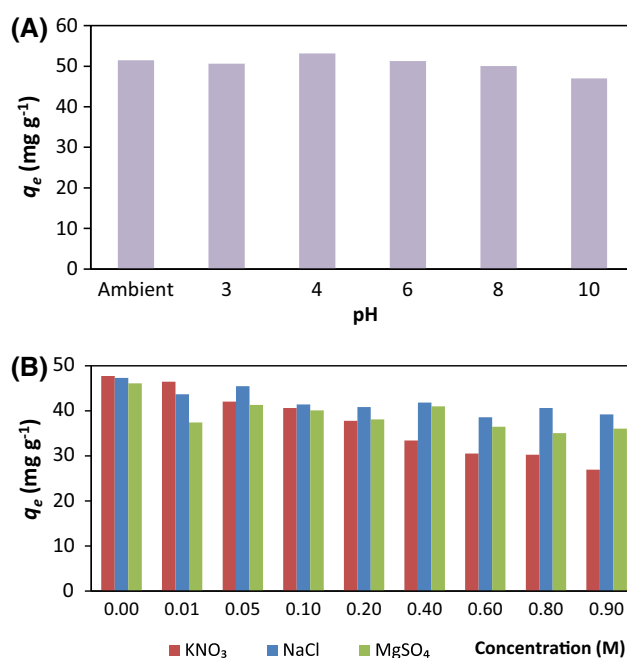

Fig. 6 Effect of **a** pH, and **b** various concentrations of KNO$_3$, NaCl and MgSO$_4$, on the removal of 100 mg L^{-1} MV by *AP* at dosage of 0.04 g *AP*/20 mL dye

The reduction in q_e is due to the suppression of the electrostatic interaction by the cations (K^+, Na^+ and Mg^{2+}) which compete with the dye molecules for the negatively charged sites on *AP* surface [37]. These reduction may give an idea on the amount of dye molecules adsorbed due to electronic attraction. Albeit the supression of electronic interaction between *AP* and MV, the q_e is not zero which indicate that hydrophobic–hydrophobic interaction and hydrogen bonding may be the major force of dye interaction with the adsorbent.

On the positive side, the ability of *AP* to maintain high removal in high ionic strength condition can be advantageous in treatment of textile wastewater, as the textile wastewater can contain high level of Na, K and Mg salts resulted from chemical salts used for pretreatment of fabrics such as surfactants and electrolytes, and detergent for washing [40].

Isotherm Studies

Three adsorption isotherm models: Langmuir [41], Freundlich [42] and Dubinin-Radushkevich (D-R) [43], were used for describing the sorption of MV onto the adsorbent.

The Langmuir isotherm is the most commonly used isotherm model which assumes that adsorption occurs homogeneously on the surface of the adsorbent resulting in monolayer and no further adsorption can occur once the adsorption site is occupied.

The equation of the Langmuir isotherm is as follows:

$$\frac{C_e}{q_e} = \frac{1}{K_L q_m} + \frac{C_e}{q_m} \tag{11}$$

where q_m is the maximum monolayer adsorption capacity of the adsorbent (mg g^{-1}), and K_L is the Langmuir adsorption constant (L mg^{-1}) which is related to the free energy of adsorption.

The separation factor (R_L) is a dimensionless constant which is an essential characteristic of the Langmuir model. The equation of R_L is expressed as:

$$R_L = \frac{1}{(1 + K_L C_o)} \tag{12}$$

where C_o (mg L^{-1}) is the highest initial dye concentration. R_L indicates if the isotherm is unfavourable ($R_L > 1$), linear ($R_L = 1$), favourable ($0 < R_L < 1$), or irreversible ($R_L = 0$).

The Freundlich isotherm model assumes multilayer coverage of adsorbate onto the adsorbate-saturated adsorbent surface.

The Freundlich isotherm equation is as follows:

$$\ln q_e = \frac{1}{n_F} \ln C_e + \ln K_F \tag{13}$$

where K_F (mg$^{1-1/n}$ L$^{1/n}$ g^{-1}) is the adsorption capacity of the adsorbent and n_F (Freundlich constant) indicates the favourability of the adsorption process. The adsorption process is considered favourable if $1 < n_F < 10$.

D-R isotherm assumes no homogenous surface of the adsorbent and is temperature-dependent. The equation is as followed:

$$\ln q_e = \ln q_m - K_{DR} \varepsilon^2 \tag{14}$$

where q_m is the saturation capacity (mg g^{-1}), K_{DR} is a D-R constant (mol^2 kJ^{-2}), and ε is the D-R isotherm constant which is also known as the Polanyi potential.

The D-R isotherm constant, ε, is expressed as:

$$\varepsilon = RT \ln\left[1 + \frac{1}{C_e}\right] \tag{15}$$

where R is the gas constant (8.314×10^{-3} kJ mol^{-1} K^{-1}) and T is temperature (K).

The mean free energy, E (kJ mol^{-1}), of the sorption per molecule of adsorbate is obtained from K_{DR}, and the equation is expressed as:

$$E = \frac{1}{\sqrt{2K_{DR}}} \tag{16}$$

The linear plots of the Langmuir, Freundlich and D-R isotherm were obtained by plotting:

C_e/q_e versus C_e, $\ln q_e$ versus $\ln C_e$, and $\ln q_e$ versus ε^2, respectively.

The parameters of the isotherm models and the error analysis are summarised in Table 3. It can be observed that the R^2 value is the highest for Langmuir isotherm when compared with Freundlich and D-R isotherm models for all the temperature. Moreover, the error analysis functions (χ^2, EABS, ARE and MSDP) of the Langmuir isotherm also displayed the smallest values, which indicate that the $q_{e,cal}$ of the Langmuir isotherm is closest to the $q_{e,\text{exp}}$. Therefore with consideration of the R^2 and the error functions, it is concluded that the Langmuir isotherm best fitted the experimental data.

The R_L values of the Langmuir isotherm for all the temperatures are between 0 and 1, which indicated that the adsorption process between MV and AP is favourable.

The low values of K_F from the Freundlich isotherm and the low q_m and E predicted from the D-R isotherm were probably due to the poor fitting of the experimental data.

The predicted q_m from the Langmuir model at ambient temperature is 194.2 mg g^{-1}, while at 65 °C the value increased to 323.4 mg g^{-1}, which could be due to the swelling of the adsorbent particle that lead to an increase in surface area at higher temperature [44]. As summarised in Table 4, AP is a better adsorbent for removal of MV than many of the agricultural residues, but its adsorbent capacity is lower when compared to Pu-erh tea, duckweed (a floating aquatic macrophyte) and synthetic adsorbent (Fe$_3$O$_4$ magnetic nanoparticle) at ambient temperature.

Thermodynamic Studies

Thermodynamic parameters such as the Gibbs free energy (ΔG^o), enthalpy (ΔH^o) and entropy (ΔS^o) were investigated by studying the adsorption process at temperature of 25, 35, 45, 55 and 65 °C.

The Van't Hoff equation was used to calculate the thermodynamic parameters which are expressed as:

$$\Delta G^O = \Delta H^O - T\Delta S^O \tag{17}$$

The Gibbs free energy is expressed as:

$$\Delta G^O = -RT \ln K \tag{18}$$

$$K = \frac{C_s}{C_e} \tag{19}$$

where K is the distribution coefficient for adsorption, C_S is the adsorbate concentration adsorbed by AP after equilibrium (mg L^{-1}), C_e is the adsorbate concentration remaining in solution after equilibrium (mg L^{-1}), R is the gas constant (J mol^{-1} K^{-1}) and T is the temperature (K).

By integrating Eq. (18) into (17), the following equation is obtained:

$$\ln K = \frac{\Delta S^o}{R} - \frac{\Delta H^o}{RT} \tag{20}$$

The values of ΔH^o and ΔS^o can be obtained from the linear plot of $\ln K$ versus T^{-1}.

Table 3 Parameters of the Langmuir, Freundlich and Dubinin-Radushkevich isotherm and the error functions analysis

Langmuir isotherm					
T (K)	298.15	308.15	318.15	328.15	338.15
q_m (mg g^{-1})	194.2	234.3	280.4	291.3	323.4
K_L (L mg^{-1})	0.066	0.056	0.049	0.048	0.041
R_L	0.014	0.017	0.023	0.022	0.023
R^2	1.000	0.994	0.997	0.995	0.990
χ^2	20.2	18.6	27.5	45.0	37.6
EABS	77.4	98.9	101.9	156.4	141.0
ARE	14.2	17.9	20.7	20.8	21.7
MSDP	36.1	36.2	34.4	29.6	38.5
Freundlich isotherm					
K_F (mg$^{1-1/n}$ L$^{1/n}$ g^{-1})	19.3	18.6	17.4	20.0	18.6
n_F	2.515	2.163	2.026	1.944	1.830
R^2	0.818	0.852	0.853	0.862	0.855
χ^2	160.6	181.4	166.6	185.8	261.1
EABS	307.0	399.4	391.0	408.9	476.0
ARE	31.7	39.6	40.5	37.8	41.1
MSDP	63.7	62.7	62.9	56.4	64.8
Dubinin-Radushkevich isotherm					
q_m (mg g^{-1})	104.8	165.8	175.7	163.4	197.6
K_{DR} (mol^2 kJ^{-2})	0.274	0.281	0.274	0.131	0.191
E (kJ mol^{-1})	1.350	1.334	1.352	1.952	1.618
R^2	0.793	0.917	0.948	0.831	0.894
χ^2	1326.6	2335.0	3058.8	3878.2	4784.9
EABS	803.7	789.2	822.4	1006.1	1095.5
ARE	163.3	231.4	270.6	302.1	328.9
MSDP	263.8	422.3	494.0	562.7	621.3

Table 4 Comparison of q_m for MV adsorption by various adsorbent

Adsorbent	q_m (mg g^{-1})	T (°C)	Reference
Azolla pinnata (AP)	194.2	Ambient	This work
AP	234.3	35	This work
AP	280.4	45	This work
AP	291.3	55	This work
AP	323.4	65	This work
Rice hull char	48.7	Ambient	[9]
Soybean straw char	70.4	Ambient	[9]
Acid modified activated carbon	83.3	30	[45]
Peanut straw char	101.0	Ambient	[9]
Artocarpus odoratissimus fruit skin	137.3	Ambient	[13]
Casuarina equisetifolia needle	165.0	Ambient	[7]
Water lettuce	267.6	Ambient	[46]
Pu-erh tea	285.7	Ambient	[47]
Duckweed *(Lemna minor)*	332.5	Ambient	[48]
Fe_3O_4 magnetic nanoparticle	416.7	Ambient	[49]

The calculated $\Delta G°$ were −7.11, −8.21, −9.16, −9.76 and −10.39 kJ mol^{-1} for 25, 35, 45, 55, and 65 °C, respectively. Increasing temperature resulted in more negative Gibbs energy which indicate the adsorption process of MV into AP is more spontaneous at higher temperature. The $\Delta H°$ was 17.2 kJ mol^{-1} and the positive value indicate that the adsorption process is endothermic, where heat is gained from the surroundings. The $\Delta S°$ value was

0.08 kJ mol^{-1} K^{-1} where the positive value indicates an increase in randomness at the solid–liquid interface during the process. Positive $\Delta S°$ value also indicates possibility of significant change in the internal structure of the adsorbent [50, 51].

The activation energy (E_a) of the adsorption process is calculated by using the Arrhenius equation, which is expressed as:

$$\ln K_2 = \ln A - \frac{E_a}{RT} \tag{21}$$

where K_2 is the pseudo 2nd order rate constant (g mg^{-1} min^{-1}), A is the Arrhenius factor, R is the gas constant, T is temperature (K) and E_a is the activation energy (kJ mol^{-1}).

E_a was estimated from the linear plot of ln K_2 versus T^{-1}, where value between 5 and 40 kJ mol^{-1} indicates physical sorption process, while 40–800 kJ mol^{-1} indicates a chemical sorption process [27]. K_2 values obtained for the removal of 100 mg L^{-1} MV at temperature of 25, 35, 45, 55 and 65 °C were 0.003, 0.005, 0.013, 0.025 and 0.034 g mg^{-1} min^{-1}, respectively. The value of E_a was found to be 54.8 kJ mol^{-1}, which indicates that the adsorption process may be controlled by chemical process.

Regeneration

To further investigate the capability of AP as adsorbent for MV removal, the regeneration experiment was carried out. The result of the regeneration experiment is summarised in Fig. 7.

Water and acid washing showed gradual reduction in removal of MV with every progressive cycle while only a small variation was observed for washing with NaOH. At the fifth cycle, water and acid washing resulted in MV removal of 47.1 and 51.2 %, respectively, while NaOH-washing resulted in 92.0 % removal when compared to the original removal at 95.9 %. The overall regenerative performance by water and acid washing varied very little and NaOH resulted in the highest regeneration capability of the adsorbent. The reason NaOH successfully regenerated the absorbent may be due to the removal of natural fats, waxes and low molecular weight lignin compounds from the surface of the adsorbent by the base while exposing chemical-reactive functional groups, such as the hydroxyl groups, which may be responsible for removal of dye molecules.

Pre-treatment of Adsorbent

Pre-treatment of adsorbents have been known to enhance their adsorption capacity towards dyes [25]. Here, AP was subjected to various treatment in order to investigate if such chemical treatment could enhance its adsorption
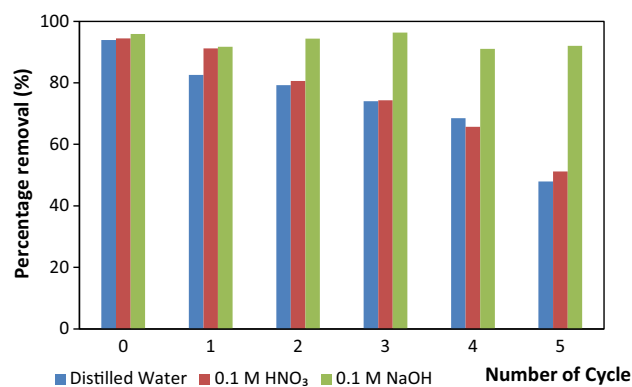

Fig. 7 Regeneration experiment of AP washed with three different solvent: Distilled water, 0.1 M HNO$_3$ and 0.1 M NaOH. *Cycle 0* represents the MV removed by the AP prior to the washing

capacity towards MV dye. The q_e of untreated, oxalic acid, citric acid, phosphoric acid and NaOH-treated adsorbent were 79.8, 47.9, 46.4, 45.6 and 71.3 mg g^{-1}, respectively, where the untreated adsorbent lead to the highest dye removal. Modification with NaOH yielded almost similar q_e with untreated AP, which may be due to exposure of favourable chemical-active groups for removal of MV as explained in the regeneration section. Modification with the acids did not improve the removal of MV, and it may be due to the removal of certain soluble organic compounds [52] that favour the removal of MV. It was reported that not all modifications of adsorbent lead to higher adsorption capacities [53].

Conclusions

The capability of AP as a potential adsorbent for the removal of MV was studied in a batch adsorption system. The optimum adsorbent dosage was 0.04 g/20 mL dye and the contact time to reach equilibrium was approximately 120 min. Optimum pH for the removal of MV is 4.0, however, no pH adjustment was made in the rest of the experiments as the removal between pH 4.0 and the ambient pH are comparable. The study of pH and ionic strength indicate that electronic interaction and hydrophobic–hydrophobic interaction may be the major forces of dye interaction. Pseudo 2nd order model best fit the kinetic data which suggested that the adsorption process was governed by chemical process. Weber-Morris model indicated that the rate-limiting step of the diffusion mechanism was not intraparticle diffusion, while the Boyd model suggested film diffusion may be the rate-limiting step or in combination of other mechanisms. The Langmuir isotherm best-fitted the experimental data with q_m of 194.2 mg g^{-1} at 25 °C and 323.4 mg g^{-1} at 65 °C, thus the increase in

temperature leads to significant improvement of dye absorption. Thermodynamic studies showed that the adsorption process is endothermic, spontaneous and has significant changes to the internal structure of adsorbent. The estimated activation energy determined using the Arrhenius equation is 54.8 kJ mol^{-1}, which indicates that the adsorption process may be controlled by chemical process. While regeneration experiment showed that NaOH managed to regenerate the adsorbent with the retention of high adsorption capability almost similar to the unused adsorbent after five cycles. Modifications of adsorbent with various chemical reagents, showed that untreated *AP* still lead to the highest removal of dye.

References

1. Rajeshwarisivaraj, Sivakumar, S., Senthilkumar, P., Subburam, V.: Carbon from Cassava peel, an agricultural waste, as an adsorbent in the removal of dyes and metal ions from aqueous solution. Bioresour. Technol. **80**, 233–235 (2001)

2. Rahchamani, J., Mousavi, H.Z., Behzad, M.: Adsorption of methyl violet from aqueous solution by polyacrylamide as an adsorbent: isotherm and kinetic studies. Desalination **267**, 256–260 (2011)

3. Srinivasan, A., Viraraghavan, T.: Decolorization of dye wastewaters by biosorbents: a review. J. Environ. Manage. **91**, 1915–1929 (2010)

4. Slokar, Y.M., Le Marechal, A.M.: Methods of decoloration of textile wastewaters. Dyes Pigments **37**, 335–356 (1998)

5. Wang, Z., Xue, M., Huang, K., Liu, Z.: Textile dyeing wastewater treatment. In: Hauser, P.J. (ed.) Advances in treating textile effluent, pp. 5–116. InTech, Rijeka (2011)

6. Rafatullah, M., Sulaiman, O., Hashim, R., Ahmad, A.: Adsorption of methylene blue on low-cost adsorbents: a review. J. Hazard. Mater. **177**, 70–80 (2010)

7. Dahri, M.K., Kooh, M.R.R., Lim, L.B.L.: Removal of methyl violet 2B from aqueous solution using casuarina equisetifolia needle. ISRN Environ. Chem. **2013**, 8 (2013)

8. Lim, L.B.L., Priyantha, N., Tennakoon, D.T.B., Zehra, T.: Sorption characteristics of Peat of Brunei Darussalam. II: interaction of aqueous copper(II) species with raw and processed peat. J. Ecotechnol. Res. **17**, 45–49 (2013)

9. Xu, R., Xiao, S., Yuan, J., Zhao, A.: Adsorption of methyl violet from aqueous solutions by the biochars derived from crop residues. Bioresour. Technol. **102**, 10293–10298 (2011)

10. Nawaz, S., Bhatti, H.N., Bokhari, T.H., Sadaf, S.: Removal of Novacron Golden Yellow dye from aqueous solutions by low-cost agricultural waste: batch and fixed bed study. Chem. Ecol. **30**, 52–65 (2013)

11. Sadaf, S., Bhatti, H., Nausheen, S., Noreen, S.: Potential use of low-cost lignocellulosic waste for the removal of direct violet 51

from aqueous solution: equilibrium and breakthrough studies. Arch. Environ. Contam. Toxicol. **66**, 557–571 (2014)

12. Sadaf, S., Bhatti, H.N., Nausheen, S., Amin, M.: Application of a novel lignocellulosic biomaterial for the removal of Direct Yellow 50 dye from aqueous solution: batch and column study. J. Taiwan Inst. Chem. Eng. **47**, 160–170 (2015)

13. Lim, L.B.L., Priyantha, N., HeiIng, C., Khairud, D.M., Tennakoon, D.T.B., Zehra, T., Suklueng, M.: Artocarpus odoratissimus skin as a potential low-cost biosorbent for the removal of methylene blue and methyl violet 2B. Desalin. Water Treat (2013). doi:10.1080/19443994.2013.852136

14. Dahri, M.K., Kooh, M.R.R., Lim, L.B.L.: Water remediation using low cost adsorbent walnut shell for removal of malachite green: equilibrium, kinetics, thermodynamic and regeneration studies. J. Environ. Chem. Eng. **2**, 1434–1444 (2014)

15. Sadaf, S., Bhatti, H.: Evaluation of peanut husk as a novel, low cost biosorbent for the removal of Indosol Orange RSN dye from aqueous solutions: batch and fixed bed studies. Clean Technol. Environ. **16**, 527–544 (2014)

16. Sadaf, S., Bhatti, H.N.: Batch and fixed bed column studies for the removal of Indosol Yellow BG dye by peanut husk. J. Taiwan Inst. Chem. Eng. **45**, 541–553 (2014)

17. Sadaf, S., Bhatti, H.N.: Equilibrium modeling for adsorptive removal of Indosol Black NF dye by low-cost agro-industrial waste: batch and continuous study. Desalin. Water. Treat. **52**, 4492–4507 (2013)

18. Conn, H.J.: Biological stains: a handbook on the nature and uses of the dyes employed in the biological laboratory, prepared with the collaboration of various members of the Biological Stain Commission. Biotech Publications, Geneva (1953)

19. Mandal, B., Vlek, P., Mandal, L.: Beneficial effects of blue-green algae and Azolla, excluding supplying nitrogen, on wetland rice fields: a review. Biol. Fert. Soils. **28**, 329–342 (1999)

20. Zehra, T., Priyantha, N., Lim, L.B.L., Iqbal, E.: Sorption characteristics of peat of Brunei Darussalam V: removal of Congo red dye from aqueous solution by peat. Desalin. Water. Treat. (2014). doi:10.1080/19443994.2014.899929

21. Tsai, S.C., Juang, K.W.: Comparison of linear and nonlinear forms of isotherm models for strontium sorption on a sodium bentonite. J. Radioanal. Nucl. Chem. **243**, 741–746 (2000)

22. Feng, Y., Dionysiou, D.D., Wu, Y., Zhou, H., Xue, L., He, S., Yang, L.: Adsorption of dyestuff from aqueous solutions through oxalic acid-modified swede rape straw: adsorption process and disposal methodology of depleted bioadsorbents. Bioresour. Technol. **138**, 191–197 (2013)

23. Sajab, M.S., Chia, C.H., Zakaria, S., Khiew, P.S.: Cationic and anionic modifications of oil palm empty fruit bunch fibers for the removal of dyes from aqueous solutions. Bioresour. Technol. **128**, 571–577 (2013)

24. Zhao, J.: Effect of surface treatment on the structure and properties of para-aramid fibers by phosphoric acid. Fibers Polym. **14**, 59–64 (2013)

25. Chieng, H.I., Lim, L.B., Priyantha, N.: Enhancing adsorption capacity of toxic malachite green dye through chemically modified breadnut peel: equilibrium, thermodynamics, kinetics and regeneration studies. Environ. Technol. (2014). doi:10.1080/09593330.2014.938124

26. Chieng, H.I., Lim, L.B.L., Priyantha, N.: Sorption characteristics of peat from Brunei Darussalam for the removal of rhodamine B dye from aqueous solution: adsorption isotherms, thermodynamics, kinetics and regeneration studies. Desalin. Water Treat. (2014). doi:10.1080/19443994.2014.919609

27. Bekçi, Z., Seki, Y., Cavas, L.: Removal of malachite green by using an invasive marine alga Caulerpa racemosa var. cylindracea. J. Hazard. Mater. **161**, 1454–1460 (2009)

28. Mane, V.S., Babu, P.: Studies on the adsorption of Brilliant Green dye from aqueous solution onto low-cost NaOH treated saw dust. Desalination **273**, 321–329 (2011)

29. Lagergren, S.: Zur Theorie der Sogenannten Adsorption gel Ster Stoffe. K. Sven. Vetenskapsakad. Handl. **24**, 1–39 (1898)

30. Ho, Y.S., McKay, G.: Pseudo-second order model for sorption processes. Process Biochem. **34**, 451–465 (1999)

31. Weber, W., Morris, J.: Kinetics of adsorption on carbon from solution. J. Sanit. Eng. Div. **89**, 31–60 (1963)

32. Boyd, G.E., Adamson, A.W., Myers Jr, L.S.: The exchange adsorption of ions from aqueous solutions by organic zeolites. II. Kinetics. J. Am. Chem. Soc. **69**, 2836–2848 (1947)

33. Zhao, Y., Yue, Q., Li, Q., Xu, X., Yang, Z., Wang, X., Gao, B., Yu, H.: Characterization of red mud granular adsorbent (RMGA) and its performance on phosphate removal from aqueous solution. Chem. Eng. J. **193**, 161–168 (2012)

34. Özacar, M., Şengil, İ.A.: Application of kinetic models to the sorption of disperse dyes onto alunite. Colloids Surf. A **242**, 105–113 (2004)

35. Maiyalagan, T., Karthikeyan, S.: Film-pore diffusion modeling for sorption of azo dye on to exfoliated graphitic nanoplatelets Indian. J. Chem. Technol. **20**, 7–14 (2013)

36. Tavlieva, M.P., Genieva, S.D., Georgieva, V.G., Vlaev, L.T.: Kinetic study of brilliant green adsorption from aqueous solution onto white rice husk ash. J. Colloid Interface Sci. **409**, 112–122 (2013)

37. Hu, Y., Guo, T., Ye, X., Li, Q., Guo, M., Liu, H., Wu, Z.: Dye adsorption by resins: effect of ionic strength on hydrophobic and electrostatic interactions. Chem. Eng. J. **228**, 392–397 (2013)

38. Al-Degs, Y.S., El-Barghouthi, M.I., El-Sheikh, A.H., Walker, G.M.: Effect of solution pH, ionic strength, and temperature on adsorption behavior of reactive dyes on activated carbon. Dyes Pigm. **77**, 16–23 (2008)

39. Samiey, B., Toosi, A.R.: Adsorption of malachite green on silica gel: effects of NaCl, pH and 2-propanol. J. Hazard. Mater. **184**, 739–745 (2010)

40. Tomasino, C.: Chemistry & technology of fabric preparation & finishing. North Carolina State University, NC (1992)

41. Langmuir, I.: The constitution and fundamental properties of solids and liquids. J. Am. Chem. Soc. **38**, 2221–2295 (1916)

42. Freundlich, H.M.F.: Over the adsorption in solution. J. Phys. Chem. **57**, 385–471 (1906)

43. Dubinin, M.M., Radushkevich, L.V.: Equation of the characteristic curve of activated charcoal. Proc. Acad. Sci. **55**, 327 (1947)

44. Forziati, F.H., Brownell, R.M., Hunt, C.M.: Surface areas of cottons and modified cottons before and after swelling as determined by nitrogen sorption. J. Res. Natl. Bur. Stand. **50**, 139 (1953)

45. Din, A.T.M., Hameed, B.H.: Adsorption of methyl violet dye on acid modified activated carbon: isotherms and thermodynamics. J. Appl. Sci. Environ. Sanit. **5**, 161–170 (2010)

46. Lim, L.B.L., Priyantha, N., Chan, C.M., Matassan, D., Chieng, H.I., Kooh, M.R.R.: Investigation of the sorption characteristics of water lettuce (WL) as a potential low-cost biosorbent for the removal of methyl violet 2B. Desalin. Water. Treat. in press, (2015) 1–11

47. Li, P., Su, Y.J., Wang, Y., Liu, B., Sun, L.M.: Bioadsorption of methyl violet from aqueous solution onto Pu-erh tea powder. J. Hazard. Mater. **179**, 43–48 (2010)

48. Lim, L.B.L., Priyantha, N., Chan, C.M., Matassan, D., Chieng, H.I., Kooh, M.R.R.: Adsorption behavior of methyl violet 2B using duckweed: equilibrium and kinetics studies. Arab. J. Sci. Eng. **39**, 6757–6765 (2014)

49. Keyhanian, F., Shariati, S., Faraji, M., Hesabi, M.: Magnetite nanoparticles with surface modification for removal of methyl violet from aqueous solutions. Arab. J. Chem. (2011). doi:10. 1016/j.arabjc.2011.04.012

50. Alkan, M., Demirbas, Ö., Dogan, M.: Adsorption kinetics and thermodynamics of an anionic dye onto sepiolite. Micropor. Mesopor. Mater. **101**, 388–396 (2007)

51. Daneshvar, E., Kousha, M., Sohrabi, M.S., Khataee, A., Converti, A.: Biosorption of three acid dyes by the brown macroalga Stoechospermum marginatum: isotherm, kinetic and thermodynamic studies. Chem. Eng. J. **195–196**, 297–306 (2012)

52. Yuan, T.-Q., Sun, R.-C.: Chapter 7.3—modification of straw for activated carbon preparation and application for the removal of dyes from aqueous solutions. In: Sun, R.-C. (ed.) Cereal straw as a resource for sustainable biomaterials and biofuels, pp. 239–252. Elsevier, Amsterdam (2010)

53. Ong, S.-T., Keng, P.-S., Lee, C.-K.: Basic and reactive dyes sorption enhancement of rice hull through chemical modification. Am. J. Appl. Sci. **7**, 447 (2010)